AIChE

A Hybrid Multiphase Flow Model

Haroun Mahgerefteh and Garfield Denton
Dept. of Chemical Engineering, University College London, London WC1E 7JE, U.K.

Yuri Rykov
Keldysh Institute of Applied Mathematics, 125047 Moscow, Russia

DOI 10.1002/aic.11569
Published online July 14, 2008 in Wiley InterScience (www.interscience.wiley.com).

The development of a hybrid model for predicting outflow following the rupture of downward sloped pressurized hydrocarbon pipelines is described. The model addresses the failure of the Method of Characteristics (MOC)-based numerical solution technique in predicting post depressurization outflow through coupling it with a hydraulic flow model. The resulting hybrid simulation is tested against the hypothetical full bore rupture of a 100-m-long, 0.158-m-diameter pipeline at various angles of decline in the range 0 to −90° containing different classes of hydrocarbons. These include a two-phase mixture, flashing liquid, liquid, and a permanent gas. The results indicate that in the case of the two-phase mixture and the permanent gas, both the MOC and the hybrid models produce very similar results with outflow being independent of the angle of decline. However, large differences in the data are obtained in the case of liquid and flashing liquid inventories with the MOC significantly under predicting outflow.
 AIChE J, 54: 2261–2268, 2008
Keywords: safety, environmental engineering, computational fluid dynamics (CFD), mathematical modeling, multiphase flow

Introduction

Pressurized pipelines are increasingly used as the main mode of transport for large amounts of hydrocarbons across the globe. Although such mode of transportation is considered relatively safe, given their extensive use, pipeline rupture incidents occur almost on a daily basis with some leading to catastrophic consequences. An average of over 6.3 million gallons of oil and other hazardous liquids is reported to be released from pipelines each year, more than half the amount released from the Exxon Valdez disaster.[1] Pipeline rupture incidents are no longer limited to developing countries. Even in the United States, despite its stringent pipeline safety regulations,[2] data published by the US Office of Pipeline Safety[3] reveal over 2600 incidents of pipeline rupture in the past decade. These have lead to a total of 186 fatalities, 702 injuries, and $3.4 billions of property damage. The corresponding cost of the damage to the environment is immeasurable. In 2004, a gas pipeline explosion in Belgium resulted in 18 deaths and over 120 serious injuries.[4]

In most developed countries it is now a regulatory requirement to demonstrate that all the hazards associated with pipeline rupture have been quantitatively accounted for and appropriate remedial action is taken in order to bring the consequences of failure to as low as reasonably practicable. Pivotal to this is the prediction of the release rate and its variation with time in the event of pipeline rupture. This information governs all the major consequences associated with pipeline rupture including fire, explosion, dispersion, and environmental damage. It forms the basis for emergency response time as well as allowing pipeline operators and safety authorities to determine minimum safe distances to populate areas.

The modeling of the outflow following pipeline rupture represents a set of unique challenges. Pipeline rupture results in an expansion wave that propagates from the rupture plane

Correspondence concerning this article should be addressed to H. Mahgerefteh at h.mahgerefteh@ucl.ac.uk.

toward the intact end of the pipeline at the speed of sound. This wave imparts a drop in pressure which in turn results in a series of expansion waves which propagate into the disturbed fluid with an increasing negative velocity, $-u$, and decreasing speed of sound, a. These waves result in the acceleration of the fluid particles in the opposite direction at a velocity $u - a$, and hence outflow.

The development of a rigorous transient outflow model therefore requires the precise tracking of these expansion waves and their propagation as a function of time and distance along the pipeline length. This involves detailed consideration of several competing and often interacting factors including heat and mass transfer, unsteady flow, and thermodynamics. Because of the fact that the speed of sound is markedly affected by the state of the fluid which may vary as a function of time and distance along the pipeline fluid, the model must also incorporate an accurate equation of state. Due consideration must also be given to the effects of heat transfer and friction both of which are flow and phase dependent. Finally, the calculation algorithm must be capable of avoiding instabilities when encountering the rapid transitions when crossing phase boundaries.

In recent years, a considerable degree of effort in modeling such highly transient flows for hydrocarbon pressurized pipelines has been undertaken (see, for example, Refs. 5–7). Crucially, however, such work is based on the fundamentally important assumption of the so-called Homogeneous Equilibrium Model (HEM),[5–7] in which the constituent phases are assumed to be at thermal equilibrium and pressure equilibrium, traveling at the same velocity. This allows the treatment of the multiphase mixture as a single fluid with average properties in direct proportion to the percentage mass of the constituent phases, thus significantly reducing the modeling complexity and the computational workload.

Notably, recent extensive studies involving the flow of different pressurized hydrocarbons through an orifice by Richardson et al.[8] have shown that the HEM breaks down when the proportion of liquid in the two-phase mixture becomes appreciable. The model is also inapplicable in the case of flashing compressed liquids because the dissolution of vapor may not be instantaneous. For such liquid mixtures, the authors successfully predict flow rates using the Bernoulli[8] incompressible flow equation in conjunction with a suitable discharge coefficient. However, this has been possible for relatively "low" dissolved vapor compositions. Also, the transition between the applicability of the HEM as opposed to the incompressible flow model is not clear. Additionally, there is a significant range of mixtures in which neither of the two models is suitable.[8]

It is important to note that Richardson et al.[8] investigations have been confined to situations in which the diameter of the pipe work upstream of the orifice is much larger than the orifice diameter. However, in the case of catastrophic full bore pipeline rupture (FBR), the area available to flow is significantly less restricted, thus providing better opportunity for unhindered phase disengagement during depressurization. As such one would intuitively expect the HEM to perform better under such situations. Indeed, HEM-based simulated results have produced reasonably good agreement with field data for the full bore rupture of real horizontal pipelines containing flashing hydrocarbon mixtures or condensable gases.[5–7]

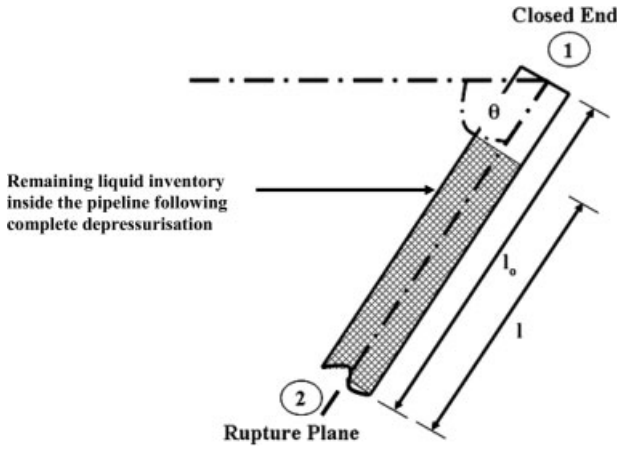

Figure 1. Schematic representation of declined pipeline showing the pertinent model parameters.

l_0, Initial height of fluid in the pipeline; l, height of fluid at time t; θ, angle of decline relative to the horizontal.

However, these tests were conducted using horizontal pipelines. In practice, long pipelines often pass through various topographies. This poses an immediate problem in the case of modeling of rupture of downward sloped or "declining" pipelines because the MOC-based simulation terminates once the line pressure has reached 1 bara. As such the gravity induced discharge of any remaining inventory in the pipeline is not accounted for. Such limitation may give rise to serious underestimations of the consequent hazard.

In this article, we report the development of a hybrid outflow model for predicting release rates following the rupture of downward sloping pipelines. The model's performance is tested against cases involving the hypothetical full bore rupture of different angled pipelines containing various classes of inventories including a two-phase mixture, flashing liquid, a permanent liquid, and a permanent gas. In each case the salient features in the data are compared and contrasted.

Theory

Full details of the background HEM outflow theory for pipeline failure is given elsewhere,[5–7] and only a brief account is given here. In the case of unsteady generalized 1D flow, the mass, momentum, and energy conservation equations for an element of a fluid within the pipeline are respectively given by[9]

$$\frac{d\rho}{dt} + \rho\frac{\partial u}{\partial x} = 0 \tag{1}$$

$$\rho\frac{\partial u}{\partial t} + \rho u\frac{\partial u}{\partial x} + \frac{\partial P}{\partial x} = \alpha \tag{2}$$

$$\rho\frac{dh}{dt} - \frac{dP}{dt} - (q_h - u\beta_y) = 0 \tag{3}$$

where ρ, u, P, and h are the density, velocity, pressure, and specific enthalpy of the homogenized pseudo fluid as a func-

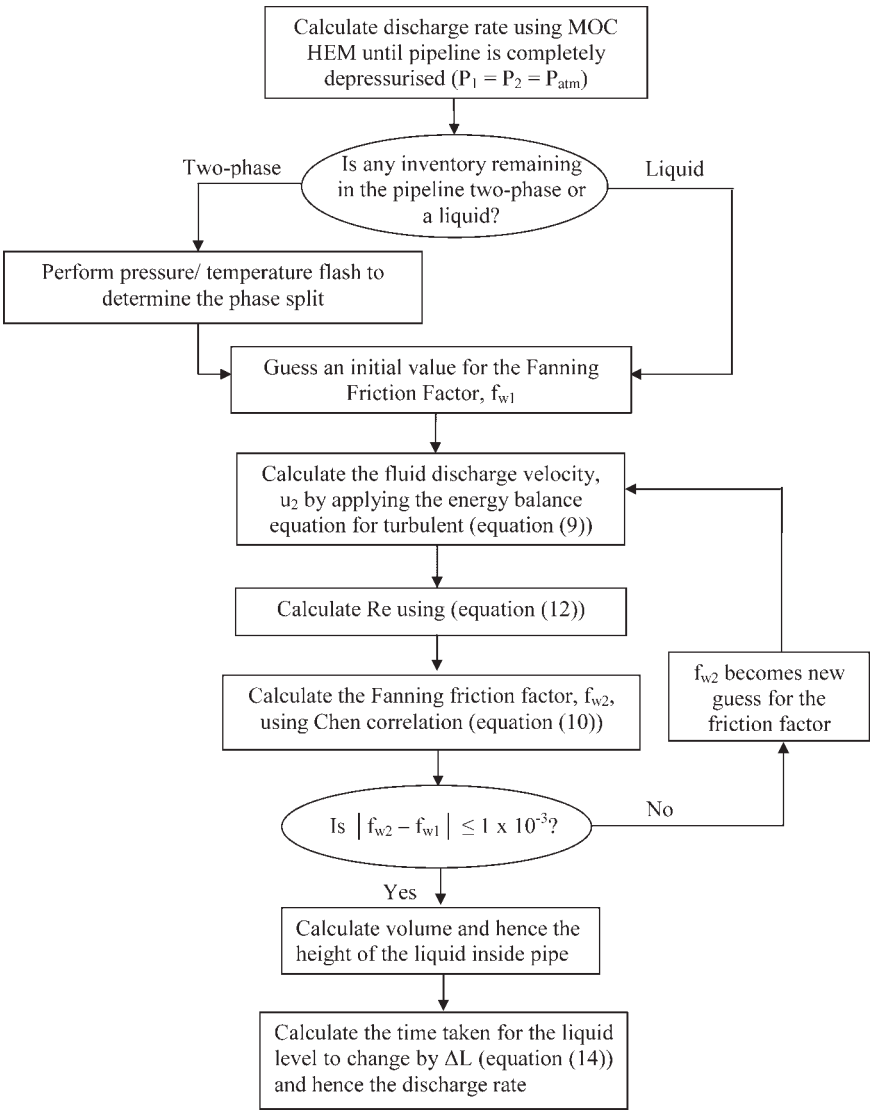

Figure 2. Hybrid Model outflow calculation algorithm.

tion of time, t, and distance, x, along the pipeline, respectively. q_h is heat transfer across the pipe wall to the fluid, whereas β_y is the friction force term given by

$$\beta_y = -2\,\frac{f_w}{D}\rho u|u| \tag{4}$$

where f_w is the Fanning friction factor and D, the pipeline diameter.

Also,

$$\alpha = -\left(\frac{2f_w\rho u|u|}{D} + \rho g\,\sin\theta\right) \tag{5}$$

where θ is the angle of inclination of the pipeline to the horizontal plane.

The solution of the above equations leads to a set of quasi linear hyperbolic equations which can only be solved numerically. The Method of characteristics (MOC)[10] has been used as the preferred numerical solution method,[5–7] as opposed to other numerical techniques such as finite difference[11,12] and finite element methods[13,14] as both have difficulty in handling

Table 1. Pipeline Characteristics and Prevailing Conditions for the Isle of Grain Pipeline Full Bore Rupture[18]

Length (m)	100
Internal diameter (mm)	154
Wall thickness (mm)	7.3
Roughness (m)	0.0005
Initial line pressure (bara)	21.6
Initial line temperature (K)	293.15
Ambient temperature (K)	292.25
Ambient pressure (bara)	1.01
Pipe wall density (kg/m^3)	7854
Pipe wall thermal conductivity [W/(m^2 K)]	53.65
Pipe wall specific heat capacity [J/(kg K)]	434
Wind velocity (m/s)	6.5
Fluid inventory (mol %)	Propane: 95% *n*-Butane: 5%

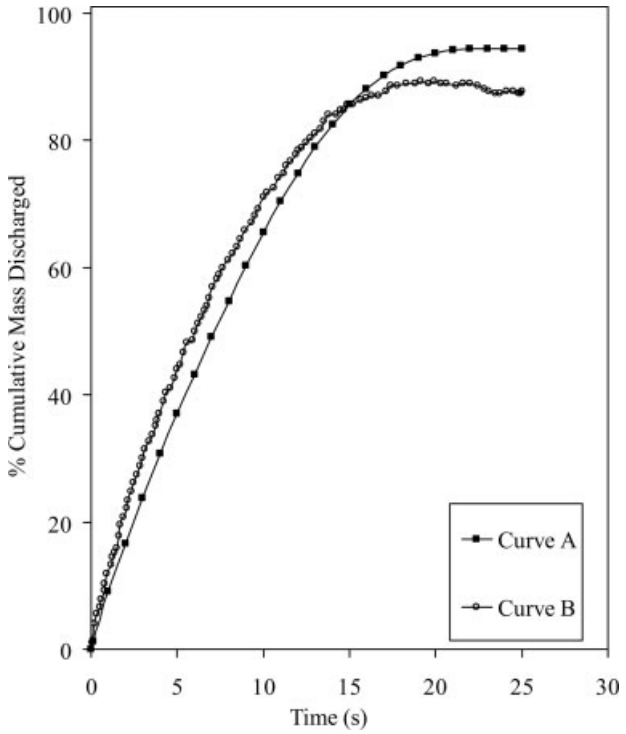

Figure 3. Variation of % cumulative mass discharged with time for the rupture of the Isle of Grain pipeline transporting 95% Propane and 5% *n*-Butane following its FBR.

Curve A: MOC HEM; Curve B: Field data; Initial line pressure: 21.6 bara; Initial line temperature: 293.15 K.

the choking condition at the rupture plane. The MOC handles choked flow intrinsically via the Mach line characteristics. Moreover, MOC is considered to be more accurate than the finite difference method as it is based on the characteristics of wave propagation. Hence, numerical diffusion associated with a finite difference approximation of partial derivatives is reduced.[15]

As mentioned earlier, the MOC outflow model terminates when the line pressure reaches 1 bara. The following describes the development of the post depressurization hydrodynamic model for predicting outflow of any remaining liquid in a declining pipeline following its failure. Figure 1 is a schematic representation of a declining pipeline showing the relevant modeling parameters under consideration.

Applying the energy balance equation across both ends of the pipeline for turbulent flow[16] gives

$$\frac{u_1^2}{2} + gl_0 \sin\theta + u(P_2 - P_1) = gl \sin\theta + \frac{u_2^2}{2} + F \qquad (6)$$

where subscripts 1 and 2 denote closed and open end conditions, respectively. Also, θ = angle of decline relative to the horizontal plane; F = energy dissipated per unit mass of fluid due to friction; l_0 = initial height of fluid in the pipeline; l = height of fluid at anytime t.

As both ends of the pipeline are at ambient pressure (pipeline is completely depressurized), $P_1 = P_2$.

Now, the energy dissipated per unit mass of fluid due to friction is given as[16]

$$F = 4\frac{R}{\rho u^2}\frac{l_0}{D}u_2^2 \qquad (7)$$

where D and R are the internal pipeline diameter and the shear stress, respectively.

The fanning friction factor, f_w, is given by

$$f_w = \frac{2R}{\rho u^2} \qquad (8)$$

Substituting f_w into Eq. 7 gives

$$F = 2f_w\frac{l_0}{D}u_2^2 \qquad (9)$$

Substituting F in Eq. 6:

$$\frac{u_2^2}{2} = g \sin\theta(l_0 - l) - 2f_w\frac{l_0}{D}u_2^2 \qquad (10)$$

Rearranging gives

$$u_2 = \left[\frac{Lg \sin\theta}{0.5 + 2f_w\frac{l_0}{D}}\right]^{1/2}, \qquad (11)$$

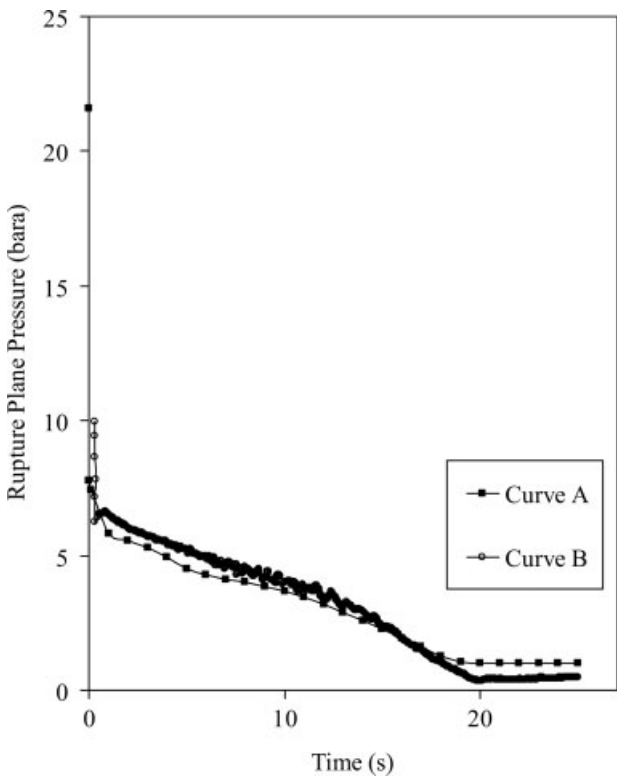

Figure 4. Variation of % rupture plane pressure with time for the rupture of the Isle of Grain pipeline transporting 95% Propane and 5% *n*-Butane following its FBR.

Curve A: MOC HEM; Curve B: Field data; Initial line pressure: 21.6 bara; Initial line temperature: 293.15 K.

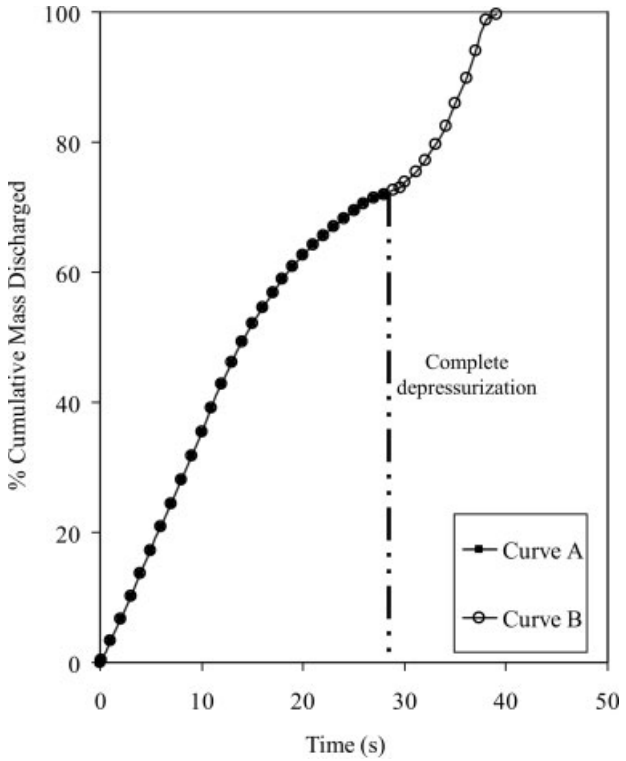

Figure 5. Variation of % cumulative mass discharged with time for the pipeline transporting 100% Butane at a decline angle of −10° following FBR.

Curve A: MOC HEM; Curve B: Hybrid Model; Initial line pressure: 21.6 bara; Initial line temperature: 293.15 K.

where $L = l_o - l$.

The fanning friction factor is calculated using the Chen correlation[17] for transition and turbulent flow through rough pipes:

$$\frac{1}{\sqrt{f_w}} = 3.48 - 1.7372 \times \ln\left[\frac{\varepsilon}{r_{in}} - \frac{16.2446}{\mathrm{Re}} \times \ln A\right] \quad (12)$$

where

$$A = \frac{\left(\frac{\varepsilon}{r_{in}}\right)^{1.0198}}{6.0983} + \left(\frac{7.149}{\mathrm{Re}}\right)^{0.8981} \quad (13)$$

ε = Pipeline roughness; r_{in} = pipeline inner radius; Re = Reynold's number,

$$Re = \frac{\rho D u_2}{\mu} \quad (14)$$

Figure 2 shows the calculation flow block diagram for determining outflow following the rupture of a pressurized pipeline based on the combined MOC HEM and the hydrodynamic model, hereby referred to as the "Hybrid Model." In essence the procedure involves the application of the MOC HEM simulation for determining outflow until 1 bara pressure equilibration along the entire pipeline length. The outflow of any remaining liquid is then determined using the above hydrodynamic model. In the case of two-phase mixtures, at 1 bara, the amount of liquid in the pipeline is determined using an isothermal flash and assuming its immediate disengagement from the vapor toward the open end of the pipeline. It is further assumed that during the post depressurization liquid outflow, the space vacated by the liquid in the pipeline is displaced by ingress of the ambient air passing through the rupture plane thus maintaining the intact end pressure at 1 bara.

Results and Discussion

The following describes the results of the application of the Hybrid MOC model for the full bore rupture of a 100-m-long, 0.154-m-i.d. pipeline containing different classes of fluids including flashing liquid, permanent liquid, two-phase mixture, and a permanent gas at 21.6 bara. For comparison, the overall pipeline dimensions including the prevailing conditions given in Table 1 are the same as those for a real horizontal pipeline ruptured by BP and Shell on the Isle of Grain[18] for which outflow data based on a pressurized liquefied petroleum gas mixture (95% Propane + 5% *n*-Butane) were recorded.

An equidistance grid system comprising 50 nodal points is employed for the simulations. The corresponding discretization time element is determined based on 90% of the Courant, Frie-

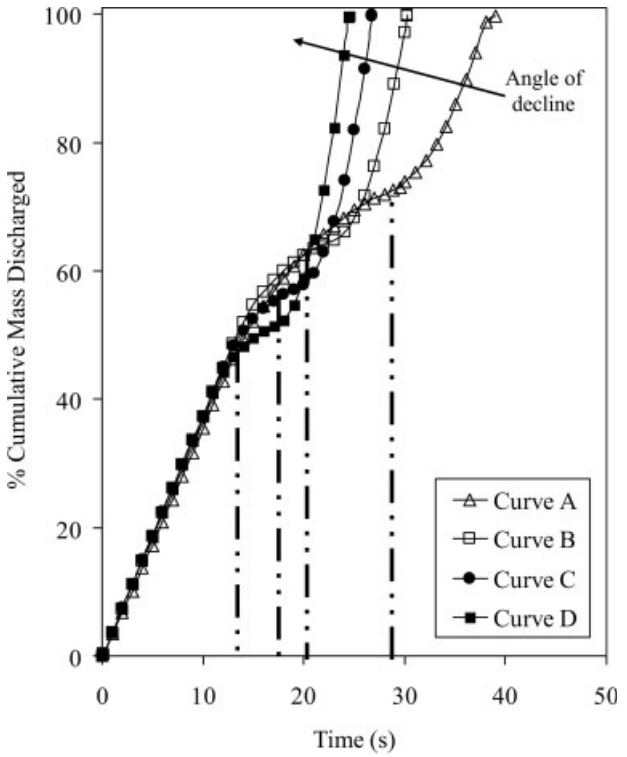

Figure 6. Variation of % cumulative mass discharged with time for a 100-m pipeline transporting 100% Butane at different angles of decline following FBR.

The dashed lines show the depressurization time to 1 bara. Curve A: −10°; Curve B: −30°; Curve C: −50°; Curve D: −90°; Initial line pressure: 21.6 bara; Initial line temperature: 293.15 K.

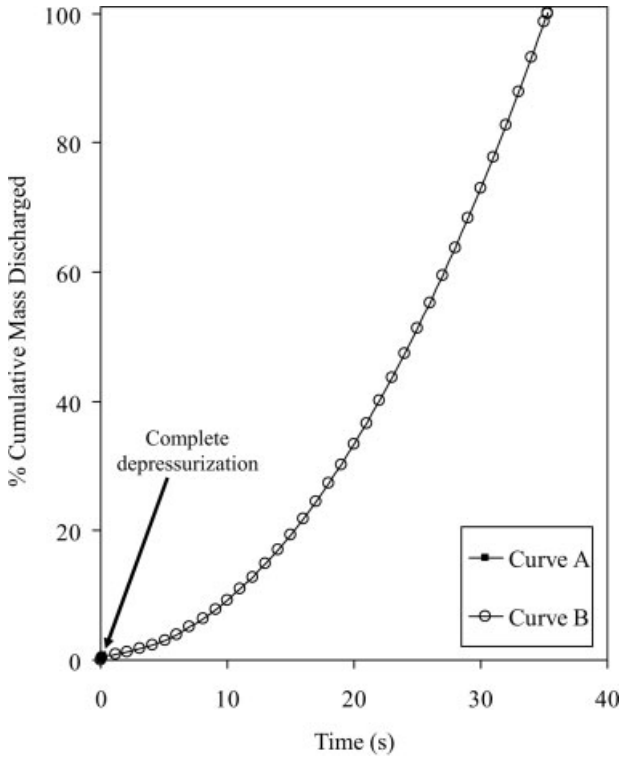

Figure 7. Variation of % cumulative mass discharged with time for the pipeline transporting 100% Hexane at a decline angle of −10° following FBR.

Curve A: MOC HEM; Curve B: Hybrid Model; Initial line pressure: 21.6 bara; Initial line temperature: 293.15 K.

drichs, and Lewy value.[10,19] The Peng Robinson equation of state[20] is used to generate the vapor–liquid equilibrium data.

Horizontal pipeline: flashing liquid

Figures 3 and 4 show the variation of the % cumulative discharge mass and rupture plane pressure with time following the full bore rupture of the actual Isle of Grain Liquefied Petroleum Gas inventory until complete depressurization to 1 bara. As it may be observed, the simulated data using MOC HEM (curve A), are in a reasonably good agreement with the measured data (curve B) during most of the depressurization period. The finite differences in the data may be attributed to the experimental errors associated with the mass (±5%) and pressure measurements (±0.5 bara) and deviations from the homogeneous equilibrium flow behavior for the two-phase mixture. The larger disagreement in the data near the tail end of the discharge process where the pressure forces begin to dissipate is consistent with the increased inapplicability of the HEM assumption. It is postulated that in this region, the liquid fraction begins to separate and lag behind the vapor due to the increased influences of friction and gravitational pull. This is consistent with the over prediction of the mass discharge by the HEM as both liquid and vapor phases are assumed to travel at the same velocity.

Figure 5 shows the variation of the % cumulative mass discharge with time following the FBR of the 100-m pipeline containing 100% liquid Butane to 1 bara at an angle of decline of −10°. Curve A shows the simulated data based on MOC HEM. Curve B on the other hand shows the outflow data predicted using the Hybrid Model as applied according to the calculation flow algorithm presented in Figure 2.

As it may be observed from Figure 5, MOC HEM simulated data (Curve A) significantly under predict the mass of fluid released from the pipeline following its full bore rupture as it ignores the post depressurization hydraulic discharge of the remaining inventory. In contrast, the Hybrid Model successfully predicts the complete discharge of the entire inventory (1133.5 kg) which is released in 39 s.

Figure 6 shows the corresponding variation of % cumulative mass discharged with time at different angles of decline following the FBR of the 100-m pipeline transporting 100% Butane. The approximate time corresponding to the complete depressurization of the pipeline to 1 bara at each angle of decline is indicated on the same figure using the dashed lines. Several important trends may be observed in the data:

(i) During the initial pressure equilibration period, the rate of cumulative mass loss remains, for the most part, independent of the angle of decline. This is consistent with the pressure forces being the dominant factor in driving out the inventory.

(ii) The post depressurization discharge rate increases with the angle of decline consistent with the increasing influence of the gravitational field effect.

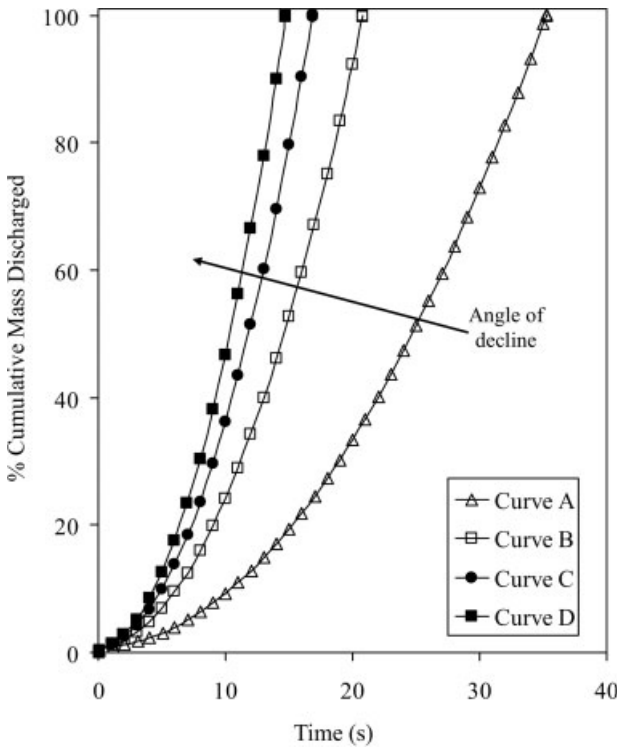

Figure 8. Variation of % cumulative mass discharged with time for a 100-m pipeline transporting 100% Hexane at different angles of decline following FBR.

Curve A: −10°; Curve B: −30°; Curve C: −50°; Curve D: −90°; Initial line pressure: 21.6 bara; Initial line temperature: 293.15 K.

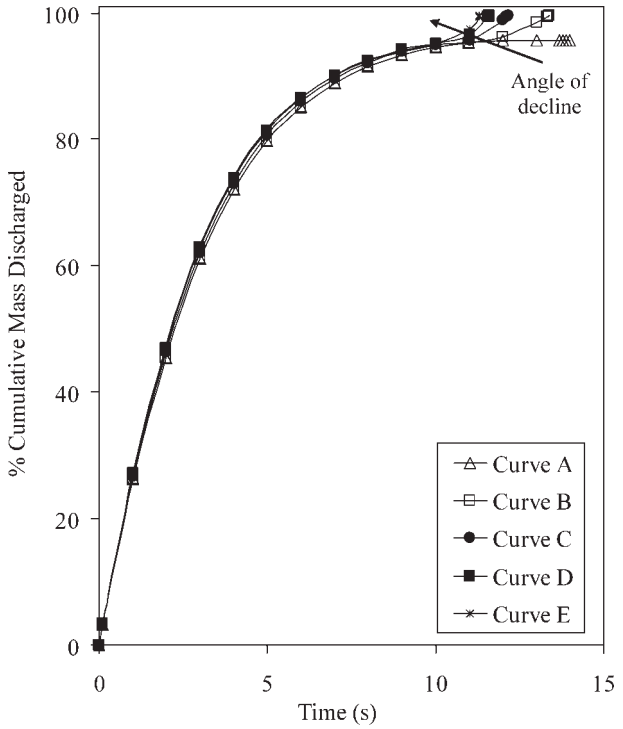

Figure 9. Variation of % cumulative mass discharged with time for a 100-m pipeline transporting 80% Hexane and 20% Methane at different angles of decline following FBR.

Curve A: −10° (MOC HEM); Curve B: −10° (Hybrid Model); Curve C: −30° (Hybrid Model); Curve D: −50° (Hybrid Model); Curve E: −90° (Hybrid Model); Initial line pressure: 21.6 bara; Initial line temperature: 293.15 K.

(iii) All the curves indicate an apparent discontinuity marked by the slowing down of the discharge rate around 1 bara followed by a rapid recovery. This is due to the assumption that the transition between the MOC HEM and hydrodynamic flow occurs after the complete depressurization of the pipeline. In practice this may happen earlier thus resulting in a higher discharge rate than that predicted. Interestingly, the extent of this transition, where the outflow remains relatively unchanged, decreases with increase in the angle of decline.

(iv) As expected the total evacuation time decreases with increase in the angle of decline.

Permanent liquid

Figure 7 presents the variation of % cumulative discharge mass with time for the 100-m pipeline containing liquid Hexane following its full bore rupture at an angle decline of −10°. Curve A shows the data based on MOC HEM, whereas curve B shows the corresponding data using the Hybrid Model.

As it may be observed from Figure 7, once again, MOC HEM (curve A) significantly under predicts the inventory released from the pipeline following its full bore rupture. Of the total 1242 kg initial inventory, only 0.7% (8.6 kg) corresponding to its expansion from 21.6 bara to atmospheric pressure is released in the first 0.2 s following pipeline failure. In contrast, the Hybrid Model successfully predicts the complete discharge of the entire inventory (1242 kg) which is released in 36 s.

Figure 8 is a plot of the % cumulative mass discharged with time at different angles of decline in the range 10–90° for the 100-m pipeline transporting 100% Hexane following its FBR. As expected, the time to completely discharge the pipeline contents dramatically decreases with increasing the angle of decline due to the increase influence of gravity.

Two-phase mixture and permanent gas

Figure 9 shows the variation of the % cumulative mass discharged with time for the 100-m pipeline containing a two-phase mixture of 80% Hexane and 20% Methane following its FBR at different angles of decline. On this occasion, both the MOC HEM and the Hybrid Model produce very similar results. This is consistent with the entire liquid content of the pipeline being discharged by the pressurized Methane by the time the pipeline reaches 1 bara. Also, the rate of depletion of the inventory during pressure equilibration is independent of the angle of decline, once again, indicating the dominant influence of the pressure forces due to the presence of the gas in the mixture. The same observation may be made in the case of the pipeline containing only methane following its

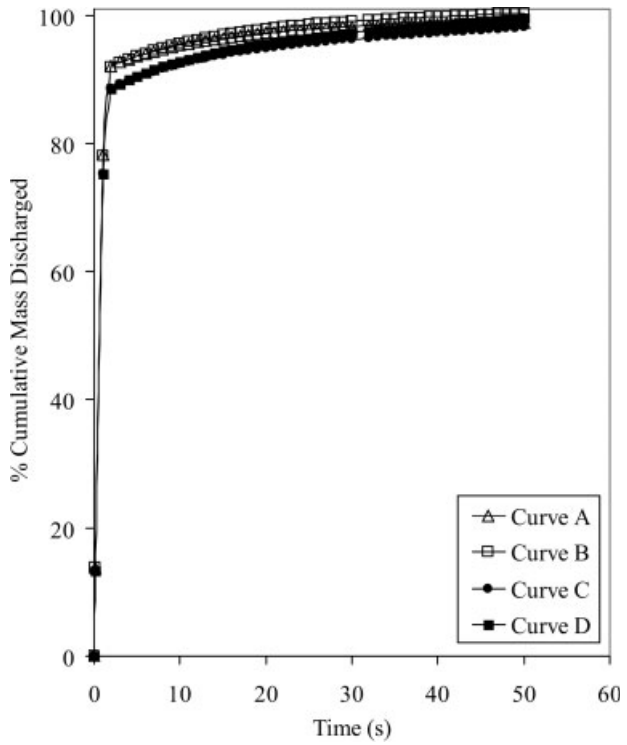

Figure 10. Variation of % cumulative mass discharged with time for a 100-m pipeline transporting 100% Methane at different angles of decline following FBR.

Curve A: −10°; Curve B: −30°; Curve C: −50°; Curve D: −90°; Initial line pressure: 21.6 bara; Initial line temperature: 293.15 K.

FBR. As indicated in Figure 10 in this case, the discharge rate is relatively independent of the angle of decline.

Conclusion

The accurate prediction of outflow following the rupture of pressurized pipelines is central to determining all the consequences associated with failure. By far the most widely accepted method for producing such data is based on the numerical solution of the conservation equation using the MOC along with the HEM assumption.

In this article, the development of a Hybrid Model based on coupling the MOC HEM with a hydrodynamic model for predicting outflow following the rupture of angled pipelines is described. The model addresses a principal limitation of the MOC HEM by accounting for the post depressurization hydrodynamic discharge.

Outflow simulation results following the full bore rupture of a 100-m-long, 0.154-m-diameter pipeline containing various classes of hydrocarbons at different angles of decline are presented and discussed.

In the case of flashing liquid inventories in declining pipelines, the MOC HEM model under predicts the amount of inventory loss as compared to the Hybrid Model as it fails to account for the discharge of the remaining liquid in the pipeline following its depressurization to 1 bara. Also, the rate of discharge prior to the pressure equilibration of the pipeline does not depend on the angle of decline. This is consistent with pressure forces as opposed to the gravitational field effect being the dominant factor in driving out the inventory during this initial period. The post depressurization discharge rate is however markedly affected by the angle of decline.

Similar trends are also observed for compressed liquids with the exception of the differences between the predictions between the two models being much more pronounced than those for the compressed volatile liquid. MOC HEM only accounts for the loss of liquid due to its finite and very rapid expansion from the line pressure to 1 bara.

In contrast, the presence of a relatively small proportion of gas in the liquid results in a dramatic change in behavior with the rate of loss of inventory no longer being dependent on the angle of decline. The results indicate that the entire liquid inventory is discharged by the gas by the time the line is depressurized to 1 bara.

Comparison with the Isle of Grain field data for the rupture of horizontal pipeline filled with LPG reveals that the homogenous equilibrium based outflow model starts to over predict the discharge rate near the tail end of the depressurization process possibly due to phase slip between the constituent gas and liquid phases.

Finally, it is important to note that pivotal to the underlying theory presented in this article are the assumptions of homogenous equilibrium flow during depressurization from the line pressure to 1 bara followed by the instantaneous disengagement and discharge of any remaining liquid from the vapor. Although comparison with the Isle of Grain data indicate the validity of the HEM during most part of the depressurization process, comparative experimental data supporting the immediate phase separation for angled pipelines do not exist. Clearly, the ideal approach would involve the development of a heterogeneous equilibrium model ascribing separate conservation equations to each constituent phase including gas, bulk liquid, and liquid droplets accounting for cross-phase concentration changes. Apart from significant increase in computational workload, such modeling work would require extensive empirically obtained data such as bubble dissolution rates, surface tension properties, and range of other flow regime dependent parameters which are not currently available. In the absence of such information, the model presented in this article represents a practical alternative from a safety point of view as it simulates the worse case scenario.

Literature Cited

1. International Chamber of Shipping, The Exxon Valdez Disaster: Ten Years After. Available at http://www.marisec.org/ics/issues/exonvald.htm.
2. United States of America Department of Transportation - Office of Pipeline Safety. OPS regulations and rulemaking. Available at http://ops.dot.gov/regs/regsindex.htm.
3. United States of America Department of Transportation - Office of Pipeline Safety.http://ops.dot.gov/stats/stats.htm.
4. HInt Dossier. *Hazards intelligence*, HInt Dossier, Tampere, Finland, 2005.
5. Mahgerefteh H, Oke A, Atti O. Modelling outflow following rupture in pipeline networks. *Chem Eng Sci*. 2006;61:1811–1818.
6. Mahgerefteh H, Oke A, Rykov Y. Efficient Numerical simulation for highly transient flows. *Chem Eng Sci*. 2006;61:5049–5056.
7. Mahgerefteh H, Oke A, Economou IG, Rycov Y. A transient outflow model for pipeline puncture. *Chem Eng Sci*. 2003;58:4591–4604.
8. Richardson SM, Saville G, Fisher A, Meredith AJ, Dix MJ. Experimental determination of two-phase flow rates of hydrocarbons through restrictions. *Trans IChemE Part B: Process Saf Environ Protect*. 2006;84:40.
9. Versteeg HK, Malalasekera W. *An Introduction to Computational Fluid Dynamics: The Finite Volume Method*. London: Prentice-Hall, 1995.
10. Zucrow MJ, Hoffman JD. *Gas Dynamics, Vols. I and II*. New York: Wiley, 1976:622–648.
11. Chen JR, Richardson SM, Saville G. A simplified numerical method for transient two-phase pipe flow. *Trans IChemE Part A*. 1993; 71:304–306.
12. Bendiksen KH, Malnes D, Moe R, Nuland S. The dynamic two-fluid model OLGA: theory and applications. *SPE Product Eng*. 1991; 6:171–180.
13. Lang E. Gas flow in pipelines following a rupture computed by a spectral method. *J Appl Math Phys (ZAMP)*. 1991;42:183–197.
14. Bisgaard C, Sorensen HH, Spangenberg S. A finite element method for transient compressible flow in pipelines. *Int J Numer Methods Fluids*. 1987;7:291–303.
15. Chen JR, Richardson SM, Saville G. Numerical simulation of full-bore ruptures of pipelines containing perfect gases. *Trans IChemE Part B*. 1992;70:59–69.
16. Coulson JM, Richardson JF. *Chemical Engineering, Vol. 1*. Oxford: Butterworth-Heinemann, 1998;18–117.
17. Chen NH. An explicit equation for friction factor in pipes. *Ind Eng Chem Fundam*. 1979;18:296.
18. Richardson SM, Saville G. *Isle of Grain Pipeline Depressurisation Tests, HSE OTH 94441*. Bootle, UK: HSE Books, HSE, 1996;1–56.
19. Courant R, Isaacson E, Reeves M. On the solution of non-linear hyperbolic differential equations by finite differences. *Commun Pure Appl Math*. 1952;5:243–255.
20. Peng DY, Robinson DB. A new two-constant equation of state. *Ind Eng Chem Fund*. 1976;15:59–64.

Manuscript received Jan. 15, 2008, and revision received Apr. 16, 2008.